

Larmor precession and Debye relaxation of single-domain magnetic nanoparticles

Zs. Jánosfalvi¹, J. Hák¹ and P.F. de Châtel^{2,1}

¹*Institute of Nuclear Research, P.O.Box 51, H-4001 Debrecen, Hungary*

²*Institute of Metal Research, CAS, Shenyang 110016, P.R. China*

The numerous phenomenological equations used in the study of the behaviour of single-domain magnetic nanoparticles are described and some issues clarified by means of qualitative comparison. To enable a quantitative *application* of the model based on the Debye (exponential) relaxation and the torque driving the Larmor precession, we present analytical solutions for the steady states in presence of linearly and circularly polarized ac magnetic fields. The power loss is calculated for both cases and the results compared with the predictions of the Landau-Lifshitz-Gilbert equation. Using the exact analytical solutions, we can confirm the insight that underlies Rosensweig's introduction of the "chord" susceptibility for an approximate calculation of the losses. We also find that this approximation provides satisfactory numerical accuracy up to magnetic fields that would generate 3/4 of the saturation magnetization if applied constantly.

PACS numbers: 47.65.Cb, 75.30.Cr, 75.75.Jn

I. INTRODUCTION

Enduring interest in colloidal dispersions of ferro- and ferrimagnetic nanoparticles is fuelled by their medical applications. Colloids of small particles of iron oxide are used in magnetic resonance imaging (MRI)¹ as contrast agents and in hyperthermia treatment as heat-generating media.² In both cases, the nanoparticles are subjected to a time-dependent magnetic field, but the frequencies and magnetic field intensities are quite different. In the case of MRI they are determined by the resonance frequency of proton, which is 63 MHz in a field commonly used, 1.5 Tesla. In hyperthermia, medical considerations require frequencies of the order 10^5 Hz and magnetic fields of 10^{-2} Tesla. The frequency of ferrimagnetic resonance in magnetite is higher than 1 GHz at zero external field,³ so that hyperthermia takes place at frequencies way below resonance, irrespective of the applied field.

The theoretical background of the processes taking place in these applications is colorful. Various approaches are being pursued with little attention for attempts to compare and evaluate the available methods. Berger *et al.*⁴ have undertaken to compare eight phenomenological equations of motion for magnetic moments of ferro- or ferrimagnetic nanoparticles dispersed in a nonmagnetic medium. They found that the calculated line-shapes in the narrow-linewidth limit, pertaining to high temperatures, are of the Lorentzian form, irrespective of the equation of motion used, but in the case of broad resonance lines significant variations are observed. Low-temperature superparamagnetic resonance spectra proved to enable a distinction between different equations of motion, of which only the Landau-Lifshitz equation provided a satisfactory fit.

The purpose of the work reported here is a theoretical comparison of two equations of motion, the Landau-Lifshitz-Gilbert equation and the modified Bloch equation (in the nomenclature of Berger *et al.*⁴). Our focus is on hyperthermia, rather than magnetic resonance. We are seeking analytical solutions to the equations of mo-

tion in the absence of a strong static magnetic field, which give, in addition to the specific losses, some insight into the underlying physical processes.

II. EQUATIONS OF MOTION AND SIMPLIFICATIONS

The behavior of single-domain ferro- or ferrimagnetic nanoparticles in an external magnetic field has much in common with that of atomic or nuclear magnetic moments. The torque on a magnetic moment μ ,

$$\mathbf{T} = \mu \times \mathbf{B} \quad (1)$$

determines the equation of motion of the angular momentum, $d\mathbf{L}/dt = \mathbf{T}$. The gyromagnetic relation, $\mu = \gamma\mathbf{L}$ enables a closed equation for μ which, applied to the magnetic moment of unit volume, provides the equation of motion of the magnetization,

$$d\mathbf{M}/dt = \gamma\mathbf{M} \times \mathbf{B}. \quad (2)$$

Here γ is the gyromagnetic ratio. The magnetization of materials we have in mind in this work is due to the spin of electrons, accordingly $\gamma = -1.76 \times 10^{11}$ Am²/Js.

The vector product in eq.(2) implies that any change of the magnetization is perpendicular to \mathbf{M} , that is, the modulus of \mathbf{M} remains constant. Also, if \mathbf{B} is constant, $d(\mathbf{M} \cdot \mathbf{B})/dt = 0$, that is, the angle between the two vectors is constant. The only motion satisfying these conditions is a precession of \mathbf{M} around \mathbf{B} . The angular velocity of the magnetization in this *Larmor precession* is $\omega_L = \gamma\mathbf{M} \times \mathbf{B}/M_\perp$, where M_\perp is the projection of \mathbf{M} on the plane perpendicular to \mathbf{B} . The Larmor frequency is defined as a positive quantity, $\omega_L = |\gamma|B$. To reduce the potential energy, $U = -\mathbf{M} \cdot \mathbf{B}$, the contribution to $d\mathbf{M}/dt$ due to relaxation must have a component parallel with \mathbf{B} . Landau and Lifshitz⁵ have chosen a "damping

term", which evidently achieves this, being proportional to $\mathbf{M} \times (\mathbf{M} \times \mathbf{B}) = (\mathbf{M} \cdot \mathbf{B})\mathbf{M} - M^2\mathbf{B}$. The *Landau-Lifshitz equation* of motion is then

$$\frac{d\mathbf{M}}{dt} = \gamma[\mathbf{M} \times \mathbf{B} + \alpha M^{-1} \mathbf{M} \times (\mathbf{M} \times \mathbf{B})]. \quad (3)$$

The coefficient α goes under the name of "the dimensionless damping coefficient", which is something of a misnomer, because addition of the "damping term" evidently *enhances* the motion of \mathbf{M} :

$$\left| \frac{d\mathbf{M}}{dt} \right| = \gamma |\mathbf{M} \times \mathbf{B}| (1 + \alpha^2)^{1/2}. \quad (4)$$

Gilbert's approach⁶ is closer to the notion of friction, as it subtracts from the Larmor torque a torque proportional to $|d\mathbf{M}/dt|$. This is reminiscent of friction in linear motion, where a force opposite to $|d\mathbf{r}/dt|$ is introduced into the equation of motion. The analogy allows a derivation of the *Gilbert equation*,

$$\frac{d\mathbf{M}}{dt} = \gamma[\mathbf{M} \times \mathbf{B} - \eta\mu_0 \mathbf{M} \times d\mathbf{M}/dt], \quad (5)$$

by adding a Rayleigh dissipation function to the Lagrangian which describes the Larmor precession of the magnetic moment.

A comparison of the Landau-Lifshitz and Gilbert equations reveals that $d\mathbf{M}/dt$ (i) is perpendicular to \mathbf{M} in both equations and (ii) in the former it consists of two mutually perpendicular terms while in the latter this is not the case. Observation (ii) implies that decomposition of the damping term in the Gilbert equation into components parallel and perpendicular to that of the Landau-Lifshitz equation will offer a direct comparison of the two. In fact, the Gilbert equation itself provides a decomposition into components which delivers the desired transformation. Multiplying both sides of eq.(5) by \mathbf{M} and taking (i) in account yield

$$\mathbf{M} \times \frac{d\mathbf{M}}{dt} = \gamma[\mathbf{M} \times (\mathbf{M} \times \mathbf{B}) + \eta\mu_0 M^2 d\mathbf{M}/dt]. \quad (6)$$

Substituting this result in the last term of the Gilbert equation and rearranging terms lead to the *Landau-Lifshitz-Gilbert (LLG) equation*,

$$\frac{d\mathbf{M}}{dt} = \gamma(1 + \alpha^2)^{-1}[\mathbf{M} \times \mathbf{B} - \alpha M^{-1} \mathbf{M} \times (\mathbf{M} \times \mathbf{B})], \quad (7)$$

where $\alpha = \gamma\eta\mu_0 M$. Clearly, for $\alpha \ll 1$ the Landau-Lifshitz equation is a good approximation, but for the general case the $(1 + \alpha^2)^{-1}$ factor is essential to eliminate the non-physical implications of the Landau-Lifshitz equation pointed out by Kikuchi⁷ and Gilbert.⁶ Also, due

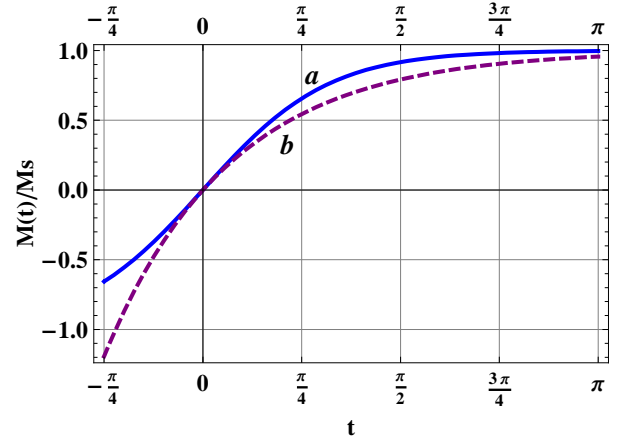


FIG. 1: (Color online) Time dependence of $M(t)/M_S$ is derived from the solution of LLG equation (7) (curve (a)) with condition $\alpha\tilde{\omega}_L = 1$. For comparison an $(1 - \exp^{-x})$ type exponential relaxation is also given (curve (b)). Both saturate to the same M_S but the path is different.

to this factor, Gilbert's damping term *reduces* the motion of \mathbf{M} :

$$\left| \frac{d\mathbf{M}}{dt} \right| = \gamma |\mathbf{M} \times \mathbf{B}| (1 + \alpha^2)^{-1/2}. \quad (8)$$

Strictly speaking, the effect of the Landau-Lifshitz and Gilbert damping coefficients cannot be described with a relaxation time, because the relaxation they stand for is not exponential. If \mathbf{B} is a constant field, pointing in the z direction, the solution of the LLG equation is $M_z = M \tanh(\alpha\tilde{\omega}_L t)$, with $\tilde{\omega}_L = \omega_L/(1 + \alpha^2)^{-1/2}$. If the magnetization is aligned perpendicular to \mathbf{B} at the outset, switching into the energetically favourable state proceeds as given in Fig.1, curve (a). For comparison, curve (b) shows the path of exponential relaxation with the same initial state. The similarity may suggest the definition of

$$\tau_{LLG} = \frac{1}{\alpha\tilde{\omega}_L} = \frac{(1 + \alpha^2)^{1/2}}{\alpha\gamma B} \quad (9)$$

as the relaxation time of the LLG dynamics. However, its dependence on \mathbf{B} would make τ_{LLG} an awkward parameter when the magnetic field is time-dependent. Furthermore, a constant value for the product $\tau_{LLG}\tilde{\omega}_L$, is counter-intuitive as different values of the ratio of the relaxation time and the Larmor precession time are expected to lead to qualitatively different behavior.

Shliomis⁸ has suggested that under well-defined conditions the equation of exponential relaxation,

$$\frac{d\mathbf{M}}{dt} = -\frac{\mathbf{M} - \mathbf{M}_{eq}}{\tau}, \quad (10)$$

should suffice to describe the behavior of a colloid of magnetic nanoparticles. Here, \mathbf{M} is the average magnetization of the particles,

$$\mathbf{M}_{eq} = M_S \mathcal{L} \left(\frac{\mu_0 H M_d V}{kT} \right) \hat{\mathbf{e}}_H, \quad (11)$$

V is the particle volume, $\hat{\mathbf{e}}_H = \mathbf{H}/H$ is the unite vector pointing along \mathbf{H} and M_S is the saturation magnetization of the colloid $M_S = \phi M_d$, where ϕ is the volume fraction and M_d is the magnetization of the single-domain magnetic nanoparticle.

The Langevin function, $\mathcal{L}(x) = \coth(x) - 1/x$, gives the magnitude of the magnetization in thermal equilibrium. Note that M_{eq} must be an ensemble average and consequently so is \mathbf{M} . In this respect, in the context of superparamagnetic resonance or hyperthermia, eq.(10) is more expedient than the LLG equation. In the latter case, having found the possible solutions of the equation of motion, one has to face the issue of the appropriate weighted average of the associated energy losses.

Clearly, the parameter τ in eq.(10) is a proper relaxation time. In a stationary field, where \mathbf{M}_{eq} is also constant, the solution of this equation for the component of \mathbf{M} along \mathbf{H} is

$$(M(t) - M_{eq}) = (M(0) - M_{eq}) \exp(-t/\tau). \quad (12)$$

In reference 9, Shliomis names eq.(10) the *Debye relaxation equation*. Yet it is often reduced from what is generally called the *Shliomis relaxation equation*,

$$\frac{d\mathbf{M}}{dt} + \mathbf{M}(\nabla \cdot \mathbf{v}) - \boldsymbol{\omega} \times \mathbf{M} = -\frac{\mathbf{M} - \mathbf{M}_{eq}}{\tau}. \quad (13)$$

Devoid of the possibility of Larmor precession, the Debye relaxation equation, eq.(10), can be looked upon as a truncated and simplified version of the Bloch-Bloembergen equation. The latter does include the gyromagnetic torque, $\mu_0 \gamma \mathbf{M} \times \mathbf{H}$. The equation of motion, which Bloch has set up for the interpretation of nuclear magnetic resonance experiments¹⁴ and Bloembergen applied to ferromagnetic resonance¹⁵ was specifically aimed at the configuration of such experiments. The z axis is aligned along the static magnetic field, which provides the axis of the Larmor precession, and enables the definition of two distinct relaxation times: τ_1 for the z component of the magnetization vector and τ_2 for its components in the xy plane. As the Debye relaxation equation is not meant to be limited to ferrofluids in a dominant static magnetic field, the simplification to a single relaxation time seems inevitable.

Usually, the equilibrium magnetization in the Bloch-Bloembergen equation is assumed to be generated by the static fields. The effect of the much weaker microwave field on the equilibrium magnetization is neglected. In what Berger *et al.*⁴ call the modified Bloch equation, the

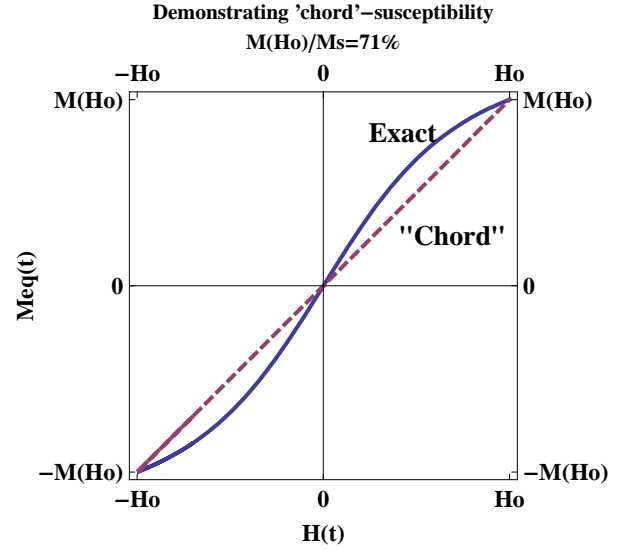


FIG. 2: Color online. The variation of exact equilibrium and 'chord'-susceptibility based magnetizations at field amplitude of $H_0 = 50$ kA/m.

equilibrium magnetization is defined in terms of the *total* effective magnetic field, which includes the microwave field as well as the internal fields (demagnetizing field and crystalline anisotropic field). The latter are reasonable, internal fields are often included in the Bloch-Bloembergen equation as well. However, the legitimacy of a time-dependent field in the same place implies the assumption that the response of the magnetization to a rapidly changing field can be described in the same way as in the case of a stationary field.

Recently, Cantillon-Murphy *et al.*¹⁶ have published a thorough analysis of the implications of the Shliomis relaxation equation for the relaxation process and energy dissipation, in superparamagnetic colloids containing magnetite nanoparticles, under the conditions of magnetic resonance imaging (MRI) and hyperthermia treatment of cancer patients.² They justify the neglect of \mathbf{v} and $\boldsymbol{\omega}$, in eq.(13) so that in fact the calculations are based on the Debye relaxation equation, eq.(10). Apart from the approximation inherent in the exclusion of the gyromagnetic torque they also applied Rosensweig's chord susceptibility,¹⁷

$$\chi_{ch} = \frac{M_S}{H_0} \mathcal{L} \left(\frac{\mu_0 H_0 M_d V}{kT} \right). \quad (14)$$

instead of the Langevin function appearing in eq.(11).

The use of the chord susceptibility in the present context is illustrated in Fig.2. As the alternating applied field is increasing towards its maximum at H_0 , eq.(11) requires the *equilibrium magnetization* to follow the concave curve denoted by \mathcal{L} , whereas the *approximate equilibrium magnetization* given by the chord susceptibility increases along the straight line between $M_{eq}(0)$ at $M_{eq}(H_0)$. The equation of that line is

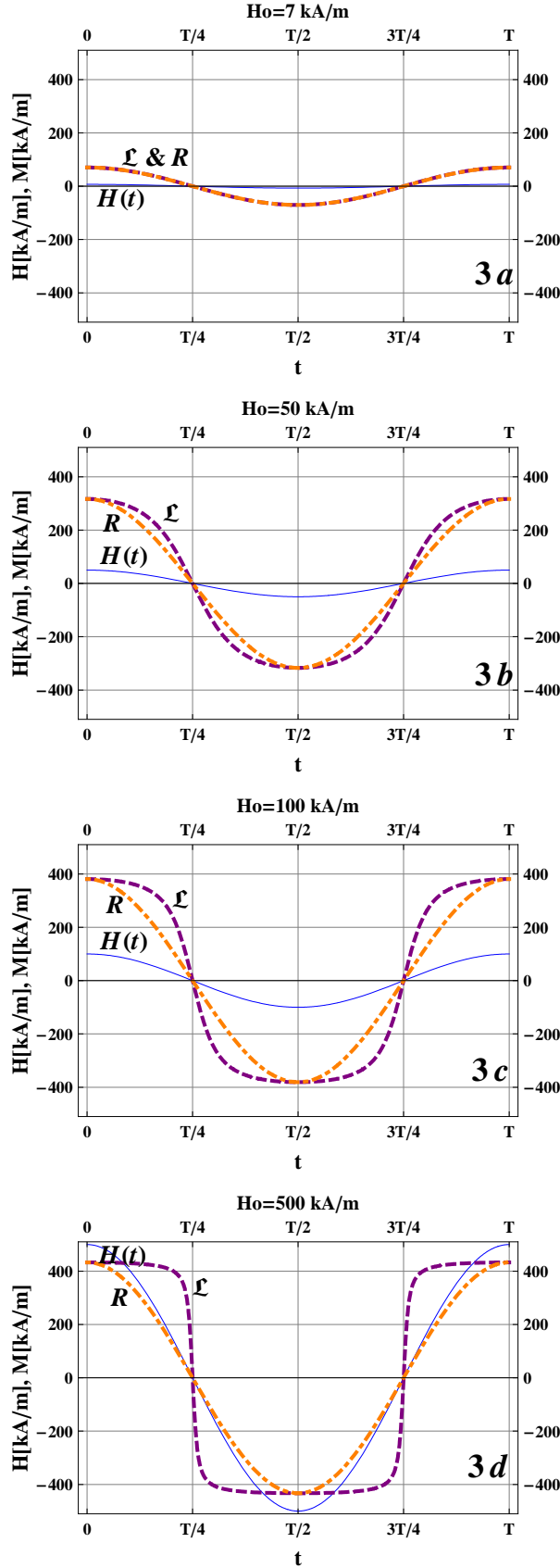


FIG. 3: (Color online) The external magnetic field dependence of the behavior of equilibrium and approximate equilibrium magnetizations for a single H cycle. The equilibrium magnetizations defined with Rosensweig's susceptibility and Langevin function are denoted by R (dotdashed) and \mathcal{L} (dashed) respectively. At weak fields the two curves are identical Fig.3(a). Increasing field strength only the extrema remain identical.

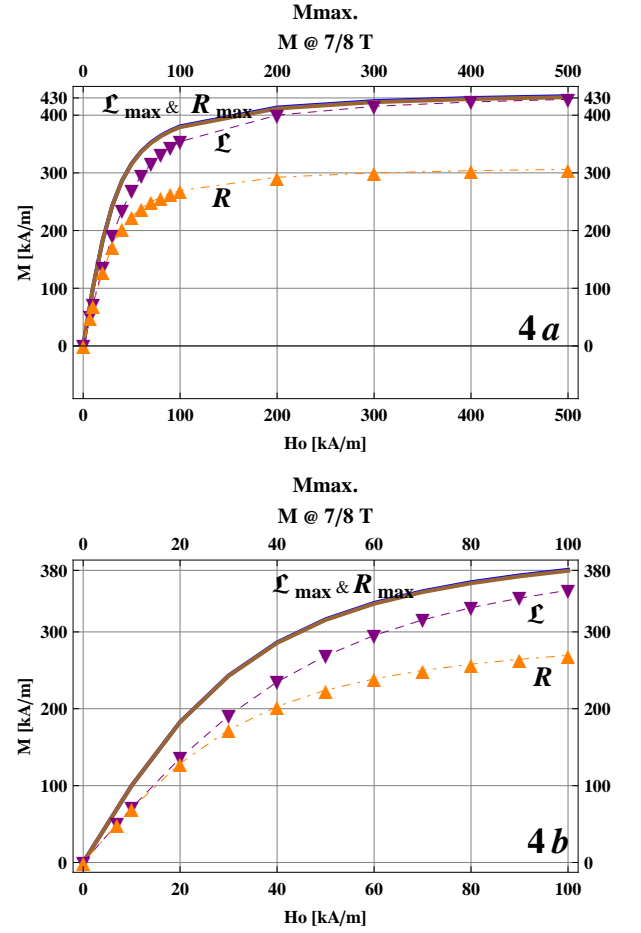


FIG. 4: (Color online) Equilibrium magnetization (\mathcal{L}) and approximate equilibrium magnetization calculated for $t = 7T/8$ and $t = T$, plotted against the amplitude H_0 of the oscillating magnetic field. At $t = T$ the two are identical by definition of χ_{ch} , but at $t = 7T/8$ the relative difference between the (\mathcal{L}) curve (down triangles) and the (R) curve (up triangles) increases with H_0 , reaching 20% at 100 kA/m.

$$M_{eq} = M_S \frac{H}{H_0} \mathcal{L} \left(\frac{\mu_0 H_0 M_d V}{kT} \right) \hat{e}_H, \quad (15)$$

hence the definition of the chord susceptibility given by eq.(14).

Equation (10) implies that in a field $H(t) = H_0 \cos(2\pi t/T)$ the relaxation pulls the magnetization towards the equilibrium magnetization, which is oscillating in time. Figure 3 shows this equilibrium magnetization determined by the Langevin function (\mathcal{L}) and the Rosensweig chord susceptibility (R). By definition of the latter, the two curves meet at $H = 0$ and $H = H_0$. In the limit of strong external field ($\mu_0 H_0 M_d V / kT \gg 1$), Fig.3(d), the \mathcal{L} curve is flipping between the extrema, while the R curve has sinusoidal characteristic. The magnetization does not exceed the saturation magnetization M_S , even for field $H_0 > M_S$. In the weak field

limit, Fig.3(a), where hyperthermia is applied, there is no difference. Figures 3(b) and 3(c) show the transition between the two behaviors. It is clear that when the field reaches a value where $M_{eq}/M_S > 0.8$ (Figs. 3(c) and 3(d)), the magnetization calculated with the chord susceptibility is substantially deviates from the correct function.

The dependence of the discrepancy between the two curves on the amplitude of the ac field is shown in Fig.4. In the low-field limit there is no discrepancy, because $\chi_{ch} = \chi$ and $M_{eq} = \chi H$, but it is visible at 20 kA/m and increases with increasing field. Beyond $H_0 = 100$ kA/m the relative difference remains constant at about 20%, which is too large to use the approximation in calculations of the magnetization. In Section IV we show that this does not disqualify the chord susceptibility in calculation of the energy loss.

In sections III and IV we present analytical solutions to the Debye relaxation equation enriched with the Larmor torque,

$$\frac{d\mathbf{M}}{dt} = \mu_0\gamma\mathbf{M} \times \mathbf{H} - \frac{\mathbf{M} - \mathbf{M}_{eq}}{\tau}, \quad (16)$$

with \mathbf{M}_{eq} as given in eq.(11). We will use these results to assess the effects of the torque on the steady-state solutions under linear and circular polarization of the ac magnetic field. As we take into account the curvature of the Langevin function, we can also discuss the implications of the chord susceptibility.

III. CIRCULAR POLARIZATION

In this section we give the analytical solution of eq.(16) for a rotating magnetic field. The first term, representing the Larmor torque, spoils the separation of Cartesian components, which has enabled the derivation of

the solution, eq.(12), found in Section II for the Debye relaxation equation. For a rotating magnetic field, $H_x = H_0 \cos(\omega t)$; $H_y = H_0 \sin(\omega t)$, the coupled equations to be solved are as follows:

$$\begin{aligned} \frac{dM_x}{dt} &= -\mu_0\gamma M_z H_0 \sin(\omega t) - \frac{1}{\tau} (M_x - M_{eq}(H_0) \cos(\omega t)); \\ \frac{dM_y}{dt} &= \mu_0\gamma M_z H_0 \cos(\omega t) - \frac{1}{\tau} (M_y - M_{eq}(H_0) \sin(\omega t)); \\ \frac{dM_z}{dt} &= \mu_0\gamma (M_x H_0 \sin(\omega t) - M_y H_0 \cos(\omega t)) - \frac{M_z}{\tau}. \end{aligned} \quad (17)$$

To handle the entanglement of the three components of \mathbf{M} , it will prove to be convenient to apply the series of transformations that enabled us in a previous work¹⁸ to solve this set of equations for free precession, i.e. in the absence of relaxation ($1/\tau = 0$). Three transformations create a coordinate system, which rotates as dictated by free Larmor precession in the rotating field. First, a rotation around the z axis by an angle $\omega\tau$ makes the xy plane follow the magnetic field, then the z axis is turned by an angle Θ into the direction of the total angular velocity $\mathbf{\Omega} = \mathbf{\omega} + \mathbf{\omega}_L$, and finally a rotation around this new, z' axis by an angle $\Omega\tau$ drives the $x'y'$ plane to rotate together with the magnetization vector. The description is reminiscent of an Euler transformation and indeed the product of the three matrices representing the rotations listed above, is of the form of the canonical Euler transformation¹⁹ with the replacements $\alpha \leftrightarrow \Omega t, \beta \leftrightarrow -\Theta$ and $\gamma \leftrightarrow -\omega t$. As the axis of the Larmor precession is the magnetic field, which rotates in the plane perpendicular to the z axis, $\mathbf{\omega}$ is perpendicular to $\mathbf{\omega}_L$ and $\Omega = \sqrt{\omega^2 + \omega_L^2}$. Also, it follows from this configuration that $\sin\Theta = \omega_L/\Omega$ and $\cos\Theta = \omega/\Omega$. In what follows, the transformation matrix will be used in the form

$$\underline{\underline{\mathbf{Q}}} = \frac{1}{\Omega} \begin{pmatrix} \omega \cos \omega t \cos \Omega t + \Omega \sin \omega t \sin \Omega t & \omega \sin \omega t \cos \Omega t - \Omega \cos \omega t \sin \Omega t & -\omega_L \cos \Omega t \\ \omega \cos \omega t \sin \Omega t - \Omega \sin \omega t \cos \Omega t & \omega \sin \omega t \sin \Omega t + \Omega \cos \omega t \cos \Omega t & -\omega_L \sin \Omega t \\ \omega_L \cos \omega t & \omega_L \sin \omega t & \omega \end{pmatrix} \quad (18)$$

To find the derivative of the transformed magnetization vector \mathbf{M}' , we need the derivative of the matrix $\underline{\underline{\mathbf{Q}}}$:

$$\frac{d\mathbf{M}'}{dt} = \frac{d\underline{\underline{\mathbf{Q}}}\mathbf{M}}{dt} = \frac{d\underline{\underline{\mathbf{Q}}}}{dt}\mathbf{M} + \underline{\underline{\mathbf{Q}}}\frac{d\mathbf{M}}{dt}. \quad (19)$$

Substituting here $\frac{d\mathbf{M}}{dt}$ from eq.(16), we find that the contribution of the Larmor torque to $\underline{\underline{\mathbf{Q}}}\frac{d\mathbf{M}}{dt}$ cancels $\frac{d\underline{\underline{\mathbf{Q}}}}{dt}\mathbf{M}$, as it should, leaving the following differential

equations for the transformed magnetization:

$$\tau \frac{d\mathbf{M}'}{dt} = -\underline{\underline{\mathbf{Q}}}\mathbf{M} + \underline{\underline{\mathbf{Q}}} \begin{pmatrix} M_{eq}(H_0) \cos(\omega t) \\ M_{eq}(H_0) \sin(\omega t) \\ 0 \end{pmatrix}. \quad (20)$$

The first term on the right-hand side gives trivially \mathbf{M}' , the second one can be found applying eq.(18), to find the differential equations for the three components of the

transformed magnetization vector. Ultimately, the analytical solution for the transformed magnetization vector

$$\begin{aligned} M'_x(t) &= \left[M'_x(0) - M_{eq}(H_0) \frac{\omega}{\Omega} \frac{\cos \delta}{\sqrt{1 + (\Omega\tau)^2}} \right] \exp(-t/\tau) + M_{eq}(H_0) \frac{\omega}{\Omega} \frac{\cos(\Omega t - \delta)}{\sqrt{1 + (\Omega\tau)^2}}; \\ M'_y(t) &= \left[M'_y(0) + M_{eq}(H_0) \frac{\omega}{\Omega} \frac{\sin \delta}{\sqrt{1 + (\Omega\tau)^2}} \right] \exp(-t/\tau) + M_{eq}(H_0) \frac{\omega}{\Omega} \frac{\sin(\Omega t - \delta)}{\sqrt{1 + (\Omega\tau)^2}}; \\ M'_z(t) &= \left[M'_z(0) - M_{eq}(H_0) \frac{\omega_L}{\Omega} \right] \exp(-t/\tau). \end{aligned} \quad (21)$$

Here δ is defined by $\sin \delta = \Omega\tau / \sqrt{1 + (\Omega\tau)^2}$, $\cos \delta = 1 / \sqrt{1 + (\Omega\tau)^2}$. Since the exponentially decaying terms are of no interest for applications on time scales exceeding τ by several orders of magnitude ($t/\tau \gg 1$) and we seek the steady-state solution in the laboratory frame, we shall drop the exponential terms. The inverse transformation is easily carried out with the transposed of matrix (18). A compact form of the final result is

$$\mathbf{M}(t) = M_{eq}(H_0) \frac{\omega}{\Omega^2} \frac{1}{1 + (\Omega\tau)^2} \begin{pmatrix} \omega \cos(\omega t) + \Omega^2 \tau \sin(\omega t) \\ \omega \sin(\omega t) - \Omega^2 \tau \cos(\omega t) \\ -\omega_L \end{pmatrix}. \quad (22)$$

Note that $|\mathbf{M}(t)| = M_{eq}(H_0) \sqrt{1 - \frac{\omega_L^2}{\Omega^2}} \frac{1}{\sqrt{1 + (\Omega\tau)^2}}$, indicating that the interplay of Larmor precession and relaxation pushes the magnitude of the magnetization, which is time-independent, below the thermal equilibrium value in a *static* field H_0 . The energy loss per cycle is easily calculated,

$$\begin{aligned} E &= -\mu_0 \int_0^{0+2\pi/\omega} \mathbf{M} \cdot \frac{d\mathbf{H}}{dt} dt \\ &= 2\pi\mu_0 M_{eq}(H_0) H_0 \frac{\omega}{\Omega} \frac{\Omega\tau}{1 + (\Omega\tau)^2}. \end{aligned} \quad (23)$$

This Debye-type dependence on $\Omega\tau$ is familiar in low-field magnetic resonance²⁰ and was shown by Garstens²¹ to be exact in the limit of vanishing static field.

The basic functional dependence of E on H_0 , ω and τ is dictated by the term $\frac{H_0\omega\tau}{1 + \Omega^2\tau^2}$. Noting, that $\omega_L^2 \sim H_0^2$, it has maximum either as a function of H_0 , ω , τ or products $\omega\tau$ and $\omega_L\tau$. To facilitate comparison with Garstens²⁰ result for frequency dependence of E , we select the dimensionless parameters $\omega\tau$ and ω_L/ω and define $n = \sqrt{\omega_L^2/\omega^2 + 1}$ and $A = \frac{\omega}{\Omega} \frac{\Omega\tau}{1 + (\Omega\tau)^2}$. Figure 5 shows A (which is proportional to E) as a function of $\omega\tau$ at various value of n . The energy loss is seen to increase with $\omega\tau$ up to a maximum at $1/n$, the value of A at the maxima being $1/(2n)$. It is remarkable how the interplay of

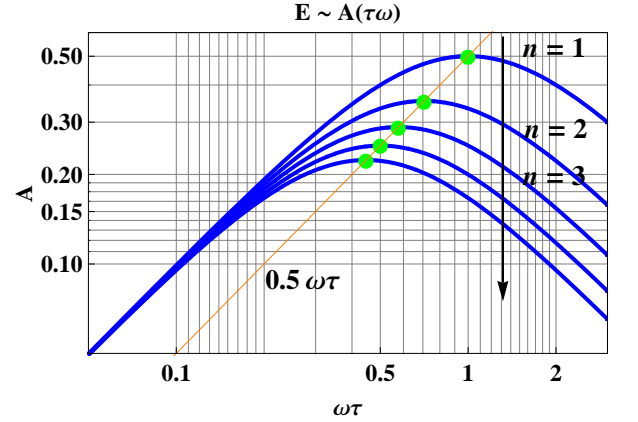


FIG. 5: (Color online) The dependence of energy $E \sim A = A(\omega\tau)$ on $\omega\tau$ for different ω_L/ω ratios as $n = 1 + \omega_L/\omega$. The curves reach maximum of $0.5n^{-1}$ at $1/n$. Largest energy dissipation is achieved at $\omega_L \ll \omega$. The maximum is shifted towards lower frequencies as n is increased, provided τ is constant.

relaxation and Larmor precession suppresses the energy loss, in the case of circular polarization.

The specific absorption rate (SAR) defined as energy loss per second and per kg, is the measure of energy losses relevant to applications:

$$SAR \doteq \frac{E\omega}{2\pi\rho} = \frac{\mu_0 M_{eq}(H_0) H_0}{\rho} \frac{\omega^2}{\Omega} \frac{\Omega\tau}{1 + (\Omega\tau)^2}. \quad (24)$$

The function describing the dependence on $\omega\tau$ and n is now

$$B = \frac{1}{\tau} \frac{\omega^2 \tau^2}{1 + n^2(\omega\tau)^2}, \quad (25)$$

which grow monotonically with $\omega\tau$, saturating at $B = \frac{1}{\tau} \frac{1}{n^2}$. Figure 6 shows that the saturation takes place at about $\omega\tau = 1$, meaning that increasing the frequency will not basically further improve the SAR.

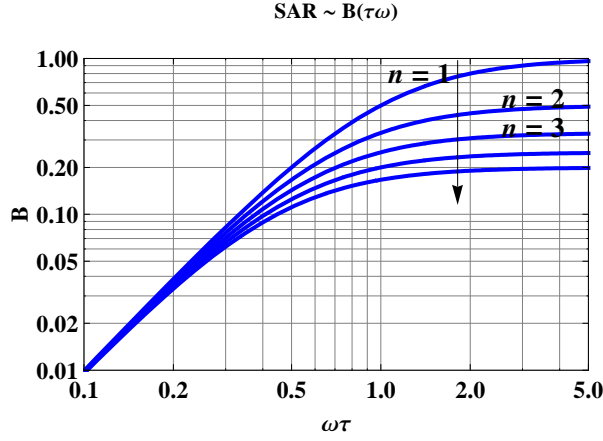


FIG. 6: (Color online) The dependence of specific absorption rate $SAR \sim B = B(\omega\tau)$ on $\omega\tau$ for different ω_L/ω ratios as $n = 1 + \omega_L/\omega$. B saturates at $\omega_L \gg 1$, however most of change takes place up to $\omega\tau = 1$. Largest specific absorption rate is achieved at $\omega_L \ll \omega$ ($n = 1$).

IV. LINEAR POLARIZATION

To find the equation of motion for the magnetization subjected to a magnetic field oscillating along the z axis, the following vectors have to be inserted into eq.(16): $\mathbf{H}(t) = (0, 0, H_0 \cos(\omega t))$, $\mathbf{M} \times \mathbf{H} = \frac{\omega_L}{\mu_0|\gamma|}(M_y \cos(\omega t), -M_x \cos(\omega t), 0)$ and $\mathbf{M}_{eq}(\mathbf{H}) = (0, 0, \phi M_d \mathcal{L}(\frac{\mu_0 M_d V H_0}{kT} \cos(\omega t)))$, where $\omega_L = \mu_0|\gamma|H_0$. The matrix of the transformation that will eliminate the Larmor term of eq.(16) depends on the sign of the gyro-magnetic ratio. For both cases we can write the matrix as

$$\underline{\underline{Q}}_{\pm} = \begin{pmatrix} \pm \sin g & \cos g & 0 \\ -\cos g & \pm \sin g & 0 \\ 0 & 0 & 1 \end{pmatrix}, \quad (26)$$

where the upper sign equals that of γ and $g(t) = (\omega_L/\omega) \sin(\omega t)$. The equation of motion for $\mathbf{M}'(t) = \underline{\underline{Q}}_{\pm} \mathbf{M}(t)$ is

$$\frac{d\mathbf{M}'(t)}{dt} = \frac{d\underline{\underline{Q}}_{\pm}}{dt} \mathbf{M} + \underline{\underline{Q}}_{\pm} \frac{d\mathbf{M}}{dt} = \frac{d\underline{\underline{Q}}_{\pm}}{dt} \mathbf{M} \pm \mu_0|\gamma| \underline{\underline{Q}}_{\pm} (\mathbf{M} \times \mathbf{H}) - \frac{1}{\tau} \underline{\underline{Q}}_{\pm} (\mathbf{M} - \mathbf{M}_{eq}(\mathbf{H})). \quad (27)$$

Taking into account that $dg/dt = \omega_L \cos(\omega t)$ (irrespective of the sign of ω_L), the first two terms in eq.(27) cancel each other. The equation of motion for $\mathbf{M}'(t)$ in terms of the new coordinate system is easy to find, as $\underline{\underline{Q}}_{\pm} \mathbf{M} = \mathbf{M}'$, by definition, and $\mathbf{M}_{eq}(\mathbf{H})$ has only a z component, which is evidently not affected by $\underline{\underline{Q}}_{\pm}$. What remains in the transformed frame is the set of equations of motion

$$\begin{aligned} \frac{dM'_x}{dt} &= -\frac{1}{\tau} M'_x; \\ \frac{dM'_y}{dt} &= -\frac{1}{\tau} M'_y; \\ \frac{dM'_z}{dt} &= -\frac{1}{\tau} \left[M'_z - M_S \mathcal{L} \left(\frac{\mu_0 M_d V H_0 \cos(\omega t)}{kT} \right) \right] \end{aligned} \quad (28)$$

The solution for the first two equations must be the familiar exponential relaxation to zero,

$$M'_{x,y}(t) = M'_{x,y}(0) \exp(-t/\tau). \quad (29)$$

Since $\underline{\underline{Q}}_{\pm}$ separates the xy plane and the z axis, the transformation back to the laboratory frame can be done in two dimensions. As g vanishes at $t = 0$, we have $M_x(0) = -M'_y(0)$ and $M_y(0) = M'_x(0)$, whence

$$\begin{aligned} \mathbf{M}(t) &= \begin{pmatrix} \pm M_y(0) \sin g + M_x(0) \cos g \\ M_y(0) \cos g \mp M_x(0) \sin g \end{pmatrix} \exp(-t/\tau) \\ &= M_{\perp}(0) \begin{pmatrix} \cos[g \mp \varphi(0)] \\ \mp \sin[g \mp \varphi(0)] \end{pmatrix} \exp(-t/\tau), \end{aligned} \quad (30)$$

where $\varphi(0)$ is the azimuth angle of $\mathbf{M}(0)$ and $M_{\perp}(0) = \sqrt{M_x^2(0) + M_y^2(0)}$. We can determine the time dependence of the angular velocity:

$$\begin{aligned} \varphi &= \tan^{-1} \frac{M_y}{M_x} = \tan^{-1} \left(\mp \tan \left(\frac{\omega_L}{\omega} \sin(\omega t) \mp \varphi(0) \right) \right) \\ &= \mp \frac{\omega_L}{\omega} \sin(\omega t) \mp \varphi(0); \\ \frac{d\varphi}{dt} &= \mp \omega_L \cos(\omega t), \end{aligned} \quad (31)$$

with the upper sign for $\gamma > 0$ and the lower sign for $\gamma < 0$. Equation (31) describes a Larmor precession whose frequency is following the time dependence of the magnetic field (note that ω_L is defined as the Larmor frequency at $H = H_0$, so that $\omega_L \cos(\omega t)$ gives the Larmor frequency at $H = H(t)$). Whether the time dependence of the precession frequency is observable will depend on the magnitude of the projection of \mathbf{M} on the xy plane, which, according to eq.(30), decays exponentially,

$$\sqrt{M_x^2(t) + M_y^2(t)} = M_{\perp}(0) \exp(-t/\tau). \quad (32)$$

If the relaxation time is very short (like in hyperthermia, where $\omega\tau \approx 10^{-4}$, the magnetization will be fully aligned along the z axis before the magnetic field undergoes a substantial change, let alone a change of sign. Of course, to observe the time dependence given in eq.(30), we also need a Larmor frequency larger than the frequency of H , that is, $\omega_L > \omega$. This condition is met in hyperthermia, at $H_0 = 200$ kA/m the Larmor frequency is about 40 GHz, whereas ω is of the order of 100 kHz.

The z component, being separated from those perpendicular to it, need not be put in a rotating frame. The search for an analytical solution to the last equation under (28) leads to a single (though not simple) integral if we substitute into eq.(28) the dM_z/dt function extracted from

$$\frac{d(e^{t/\tau} M_z)}{dt} = \frac{1}{\tau} e^{t/\tau} M_z + e^{t/\tau} \frac{dM_z}{dt}. \quad (33)$$

To avoid the difficult integral, for $\zeta =$

$\mu_0 H_0 M_d V / kT \ll 1$ one can use the susceptibility instead of the Langevin function, i.e., the first term in the Taylor series of \mathcal{L} instead of the function \mathcal{L} . In fact, the integrals can be done for higher order terms also (Ref. 22, p.228). As the Taylor series of $\coth x$ necessary here (Ref. 22, p.42) is only valid for $|x| < \pi$, the resulting expression for the time dependence of the equilibrium magnetization in terms of odd powers of $\cos(\omega t)$,

$$\mathcal{L}(\zeta \cos(\omega t)) = \sum_{m=1}^{\infty} \frac{2^{2m}}{(2m)!} B_{2m} (\zeta \cos(\omega t))^{2m-1}, \quad (34)$$

where the B_{2m} are Bernoulli numbers as defined and listed in Ref. 22, p.1040 and p.1045, respectively. Substituting the series (34) into eq.(33),

$$e^{t/\tau} M_z = \frac{M_S}{\tau} \sum_{m=1}^{\infty} \frac{2^{2m}}{(2m)!} B_{2m} \zeta^{2m-1} \int e^{t/\tau} \cos^{2m-1} \omega t dt. \quad (35)$$

Now is straightforward to find a solution to the equation of motion for M_z which is analytical, albeit in the form of an infinite series :

$$M_z = \frac{2M_S}{\tau} \sum_{m=1}^{\infty} \frac{1}{m} B_{2m} \zeta^{2m-1} \sum_{k=0}^{m-1} \frac{(1/\tau) \cos((2k+1)\omega t) + (2k+1)\omega \sin((2k+1)\omega t)}{(m-1-k)!(m+k)! [(1/\tau)^2 + (2k+1)\omega^2]} \quad (36)$$

There are three features of this solution that can be revealed without evaluating the series: (i) the exponential factors have disappeared, meaning that the function describes a steady state, (ii) keeping only the $m = 1$ term in the series the well-known result for the frequency-dependent Curie susceptibility [Ref. 11, eqs. (2) and (10)], $M_z = \chi_0 H_0 [\cos(\omega t) + \omega\tau \sin(\omega t)] / [1 + (\omega\tau)^2]$ with

$$\chi_0 = \frac{\mu_0 M_d^2 V \phi}{3kT} \quad (37)$$

emerges and (iii) the double summation is essentially a Fourier series, of which only the $k = 0$ sine terms are needed for the calculation of losses, because M_z , multiplied by $-dH(t)/dt = H_0 \omega \sin(\omega t)$, will be integrated over a cycle.

Keeping only the $k = 0$ terms in the second sum in eq.(36) amounts to eliminating the higher harmonics in the time dependence of the magnetization, which are generated due to the substantial nonlinearity of the Langevin function beyond $x \approx 0.5$. It follows then that for any value of H_0 a susceptibility can be found, which will provide the exact energy loss on the assumption that the magnetization is

$$M_z^{eff} = 2M_S \sum_{m=1}^{\infty} \frac{1}{(m!)^2} B_{2m} \zeta^{2m-1} \frac{\cos(\omega t) + \omega\tau \sin(\omega t)}{1 + (\omega\tau)^2}. \quad (38)$$

Looking back at Fig.3(d), it becomes now clear that abrupt changes of the magnetization triggered by the flipping of the equilibrium magnetization will not influence the calculated energy loss, because they are represented by high-frequency terms in M_z .

The effective magnetization of eq. (38) may be looked upon as a fictitious magnetization, which, if realized, would give the correct losses without reproducing the correct fictitious hysteresis loop. Instead, the shape of the hysteresis loop and its frequency dependence are exactly the same as those one gets at low fields, where the static magnetization is proportional to the magnetic field. Equation (38) confirms then the insight that underlies Ronsweig's introduction of the chord susceptibility [Ref.¹⁷ eq.(2)] and enables the calculation of the "field dependence" of a fictitious susceptibility. In fact, the susceptibility relevant to the energy loss, implicitly defined by $M_z^{eff} = \chi_{loss} H_0 [\cos(\omega t) + \omega\tau \sin(\omega t)] / [1 + (\omega\tau)^2]$ with

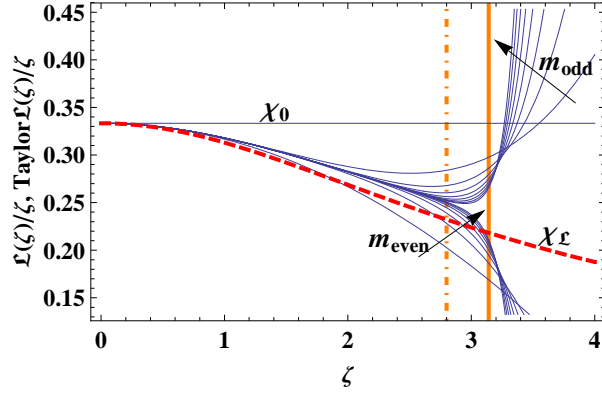


FIG. 7: (Color online) Convergence of the Taylor series expansion of $\mathcal{L}(\zeta)/\zeta$ representing the summing term in eq.(39). Thin constant line is related to $m_{max} = 1$ (χ_0), while thin curves are superposed functions up to $m_{max} = 17$. Red dashed line shows the exact $\chi_L = \mathcal{L}(\zeta)/\zeta$. Arrows point towards the direction of increasing m .

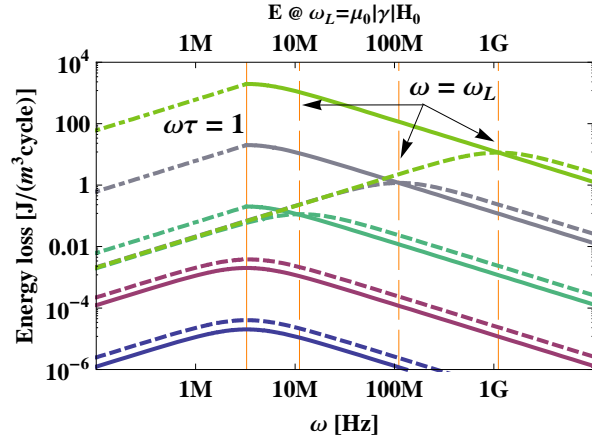


FIG. 8: (Color online) Energy loss as a function of frequency ω , parameterized by field strength H_0 . Thick lines correspond to linear polarized cases, while dashed ones to circular polarized cases. Auxiliary thin line is drawn to explore behavior around resonance $\omega\tau = 1$. There is local maximum for each circular polarized case when condition $\omega = \omega_L$ is fulfilled (Thin, dashed auxiliary lines).

$$\chi_{loss} = 2 \frac{\mu_0 H_0 M_d^2 V \phi}{kT} \sum_{m=1}^{\infty} \frac{1}{(m!)^2} B_{2m} \zeta^{2(m-1)}, \quad (39)$$

$$E = -\mu_0 \int_{t_0}^{t_0+2\pi/\omega} \mathbf{M} \cdot \frac{d\mathbf{H}}{dt} dt = -\mu_0 \int_{t_0}^{t_0+2\pi/\omega} M_z^{eff} \cdot \frac{dH_z}{dt} dt = \pi \mu_0 H_0 \chi_{loss}(\zeta) \frac{\tau \omega}{1 + (\tau \omega)^2}. \quad (40)$$

Comparing the $\omega\tau$ dependence of E in both polar-

ized cases, prompt can be realized that frequency de-

pendence of of the fictitious susceptibility χ_{loss} . Note that while the deviation of χ_{chord} from χ_0 is increasing substantially, the difference between the exact χ_{loss} and χ_{chord} is small and remains constant at about 5% even for $2 < \zeta < 2.8$. Hence for $\zeta > 1$ calculating the energy loss using χ_0 is not reliable, but close enough results can be obtained using the χ_{chord} susceptibility.

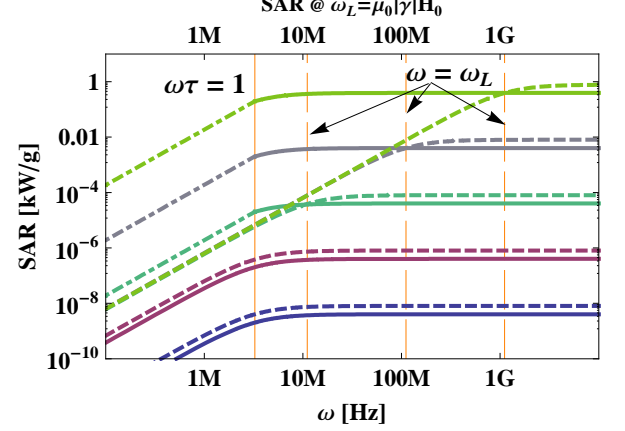


FIG. 9: (Color online) Specific absorption rate as a function of frequency ω , parameterized by field strength H_0 . Thick lines correspond to linear polarized cases, while dashed ones to circular polarized cases. Auxiliary thin line is drawn to explore behavior around resonance $\omega\tau = 1$. Maximum reached for each circular polarized case when condition $\omega > \omega_L$ is fulfilled (Thin, dashed auxiliary lines).

Calculating the energy loss per cycle,

ized cases, prompt can be realized that frequency de-

pendence of energy dissipation in circularly and linearly polarized cases can be equivalent by a factor of 2, if $n = \sqrt{\omega_L/\omega + 1} = 1$ and the linear approximation of M_{eq} is taken for both polarized cases.

At high driving field amplitudes ($\zeta \gg 1$) the energy absorption per cycle can be estimated as follows. For $\omega \ll 1/\tau$ eq.(28) implies that M_z lags behind the target $M_S \mathcal{L}(\zeta \cos(\omega t))$ value by time τ , which yields for the energy absorption $E \approx 4\mu_0 M_S H_0 \omega \tau$. For $\omega \gg 1/\tau$ according to eq.(28) the driving magnetic field causes only saw-tooth curve like oscillation of magnetization around the zero value with amplitude $\approx M_S \pi / 2\omega \tau$. The energy absorption per cycle in this case is $E \approx 4\mu_0 M_S H_0 / \omega \tau$.

V. SUMMARY AND CONCLUSIONS

Analytical solutions of Bloch-Bloembergen equation for both polarized cases are presented. They are in excellent agreement with the numerical solutions.

Differences in time-dependence of magnetization using Rosensweig's "chord" - susceptibility and Langevin function are emphasized in Figs.3 and 4, where H_0 is parameterised. Formulae for energy dissipation and specific absorption rate (SAR) are also provided. Short analysis is given for strong and weak field limit. It can be concluded that in hyperthermia region Rosensweig's suggestion for "chord" - susceptibility is reasonable. Linear approximation of Langevin function, $\mathcal{L}(x) \approx x/3$, can also be used provided the value of argument x is small enough. While $x = 0.4$ means 1% difference in linear approximation, at $x = 1.2$ already deviates with 10%.

The frequency dependence of energy dissipation and SAR is also clarified, see Figs. 5 and 6. Possible maximum of energy dissipation decreases with increasing ratio ω_L/ω and shifted to lower ω when relaxation time τ is taken constant. SAR in the high $\omega\tau$ limit shows saturation and its value is decreasing with increasing ratio ω_L/ω . Equivalence of linear and circular polarized field can be stated with a factor of two, if the Larmor frequency is negligible small to external field frequency and linear approximation of Langevin function is taken for expressing equilibrium magnetization. In Fig.8 the resulting energy loss per cycle is depicted as a function of frequency for both polarized cases as a parameter of driving field amplitude H_0 where $\tau_0 = 10^{-9}$ s and $M_S = 446$

kA/m with $r = 5$ nm nanoparticles. For small driving field amplitudes a common energy loss local maximum is observed. By increasing the driving field amplitude, the tent shape form of the energy loss curve is not changing. For the linearly polarized field it is proportionally shifted to higher energy loss values, while for the circularly polarized case the energy absorption maximum is shifted towards higher frequencies. Notably, in the latter case at the given set of parameters the energy loss at lower frequencies just started to decrease with increasing field strength (see eq.(23)).

Figure 9 shows the same data in practical units of kWg^{-1} as defined for SAR. The presented results concerning the shift of the energy dissipation maximum and high frequency behaviour are in excellent agreement with the results derived from the Landau-Lifshitz-Gilbert equation¹⁸.

Contrary the results obtained for low frequency region show different behaviour. This difference is outset by the possibility of changing the magnitude of magnetization. For example this produces resonance like $E(H_0)$ dependence in Bloch-Bloembergen case, while the lack of this possibility results in H_0 independent $E(H_0)$ behaviour in the Landau-Lifshitz-Gilbert frame for circularly polarized field. The difference in results for linearly polarized field also originates from this possibility.

At low frequency and relatively high driving field amplitudes, linearly polarized field would yield more dissipation compared to the circular case when the relaxation processes characterized by the Bloch-Bloembergen equation. Our final conclusion is alike as drawn from analyzing Landau-Lifshitz-Gilbert equation: when the relaxation process is characterized by the Bloch-Bloembergen equation, the technical complications of generating a circularly polarized field in difficult geometry need not be considered.

Acknowledgement

One of the author, Zs.J., wishes to express special thanks to I. Nándori and to colleagues in the lab for their valuable critical advices and continuous support. The authors acknowledge support from the Hungarian Scientific Research Fund (OTKA) No.101329.

-
- ¹ H.B. Na, I.C. Song and T. Hyeon, Adv. Mater. **21**,(2009), 2133.
 - ² R. Hergt, S. Dutz, R. Müller and M. Zeisberger, J. Phys.: Condens. Matter. **18**, (2006), S2919.
 - ³ P.C. Fannin, C.N. Martin, V. Soculiuc, G.M. Istratuca and A.T. Giannitsis, J.Phys. D: Appl. Phys.**36**, (2003), 1227.
 - ⁴ R. Berger, J.-C. Bissey and J. Kliava, J. Phys.: Condens. Matter. **13**, (2000), 9347.
 - ⁵ L.D. Landau and E.M. Lifshitz, Phys. Z. Sowj. **8**,(1935),

- 153.
- ⁶ T.L. Gilbert, Phys. Rev. **100** (1956) 1243, IEEE Trans. Magn. **40** (2004) 3443.
- ⁷ R. Kikuchi, J. Appl. Phys. **27** (1956) 1352.
- ⁸ M.I. Shliomis, Sov. Phys. Uspekhi, **17** (1974) 427. (УФН **122** (1974) 153).
- ⁹ M.I. Shliomis, Phys. Rev. Lett. **92** (2004) 188901.
- ¹⁰ A. Engel, H.W. Müller, P. Reimann and A. Jung, Phys. Rev. Lett. **91** (2003) 060602.

- ¹¹ C. Rinaldi, A. Chaves, S. Elborai, X. He and M. Zahn, *COCIS* **10** (2005) 141.
- ¹² R.E. Rosensweig, *J. Chem. Phys.* **121** (2004) 1228.
- ¹³ M.I. Shliomis, *Phys. Rev. E* **64** (2001) 060501.
- ¹⁴ F. Bloch, *Phys. Rev.* **70** (1946) 460.
- ¹⁵ N. Bloembergen, *Phys. Rev.* **78** (1950) 572.
- ¹⁶ P. Cantillon-Murphy, I.I. Wald, E. Adalsteinsson and M. Zahn, *J. Magn. Magn. Mater.* **322** (2010) 727.
- ¹⁷ R.E. Rosensweig, *J. Magn. Magn. Mater.* **252** (2002) 370.
- ¹⁸ P.F. de Châtel, I. Nándori, J. Hakl, S. Mészáros and K. Vad, *J. Phys. Condens. Matter.* **21** (2009) 124202.
- ¹⁹ D.A. Varshalovich, A.N. Moskalev and V.K. Khersinskii, *Quantum Theory of Angular Momentum*, World Scientific (1988)
- ²⁰ M.A. Garstens and J.I. Kaplan, *Phys. Rev.* **99** (1955) 259.
- ²¹ M.A. Garstens, *Phys. Rev.* **93** (1954) 1228.
- ²² I.S. Gradshteyn and I.M. Ryzhik, *Tables of integrals, series and products*, 7th edition, Academic Press (2007) 228.